

Three-dimensional modelling of masonry arch bridges based on predetermined planes of weakness

T. Kamiński

Wroclaw University of Technology, Institute of Civil Engineering, Wroclaw, Poland

ABSTRACT: The paper deals with an original approach to 3D analysis of masonry arch bridges. The proposed solution is based on a semi-micro-modelling of the masonry arch barrel. The arch is divided into discrete masonry segments separated with areas of weaker material comprising potential crack planes. The application of the model enables one to carry out the analysis of the ultimate limit state of structures and provides results in the form of the ultimate loads and failure modes. The examples of the analysis and fundamental results for various structural cases are described and discussed.

1 INTRODUCTION

Modelling and analysis of masonry arch bridges still remains a vital issue, as yet unsolved satisfactorily. On the one hand, there is the need to carry out such tasks due to a large number of existing structures of this type subjected to new and increased operation demands. On the other hand, solving such a complex, multi-parameter and nonlinear problem becomes a substantial difficulty in the sense of precise global formulation covering all the aspects of the structural behaviour as well as in the sense of numerical solution. In this situation a possible approach to the problem is the application of models worked out to specific types of results. Such models could simplify parameters less important for the analysis in favour of computational efficiency, but should precisely accommodate the features being essential for the sake of the considered issue. In the proposed approach the aim of the analyses is to reach the ultimate limit state and modes of the global failure without a detailed control of local stresses. Besides, to reasonably analyse the global behaviour, all main structural elements are included and a full 3D model is applied. Thus, such models have a much bigger potential to represent the behaviour of real masonry bridges than have the commonly applied 2D structure models.

2 THREE-DIMENSIONAL FE MODELS OF MASONRY BRIDGES

2.1 General remarks

The main goal of the proposed 3D model of a masonry bridge was to combine a reliable and complex analysis including transverse effects of structural behaviour with its relative simplicity enabling one to model and solve the problem with an acceptable computational effort. Therefore some simplifications in representing structural elements were applied, however the crucial areas of the structure were modelled providing its proper behaviour at the ultimate limit state.

A special care was paid to modelling of the main component – the arch barrel. The most precise discretization of this masonry element could provide the application of a detailed micro-modelling technique (proposed by Lourenco et al. 1995) considering mortar joints, masonry units and the conditions for their mutual interactions in the whole arch. Unfortunately, such

a model would be a huge and extremely time consuming numerical problem. On the other hand, a macro-modelling technique, treating masonry as a homogenous material, commonly applied in the analysis (e.g. Fanning and Boothby 2001), does not provide a good representation of the structural behaviour at the limit state. Therefore, a semi-micro-modelling, being between micro- and macro-modelling, was applied to the presented models of masonry.

2.2 Model of geometry

The presented 3D model takes into account the main structural components of a single-span masonry bridge: arch barrel, spandrel walls and backfill (Fig. 1). Geometrical dimensions of the model presented as an example correspond to typical dimensions of real structures and are as follows:

- arch span: $L_0 = 5$ m,
- arch rise: $r = 1.25$ m,
- constant arch thickness: $d = 30$ cm,
- bridge width: $B = 4$ m,
- spandrel wall thickness: $s = 24$ cm,
- height of backfill over crown: $h = 0.35$ m.

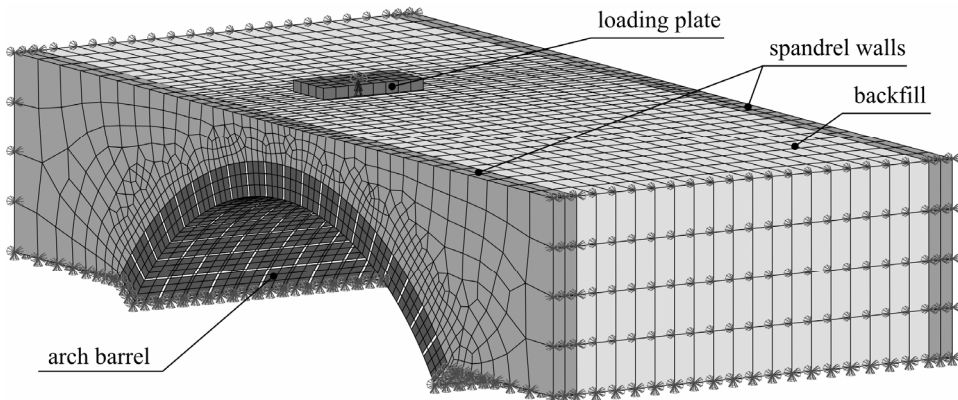


Figure 1 : A three-dimensional FE model of a masonry bridge structure.

The segmental arch barrel is rigidly supported along its springings. This assumption can be quite unrealistic for real cases but on the other hand, the stiffness of sound supports should provide a limitation to their spread to the negligible level. Along the longitudinal edges of the arch spandrel walls standing on it are modelled. The walls are extended beyond the arch to some distance where they are rigidly supported along their bottom surfaces; over the arch barrel they are connected to the nodes of the arch extrados. Over the arch barrel and between the spandrel walls a backfill is modelled. At both ends of the model the vertical boundaries of the soil and spandrel walls have imposed constraints on the horizontal displacements only.

At all boundaries between the backfill and the arch components the contact elements are used. The contact elements model the interaction between the contacting bodies by compressive and shear forces but without the tension transfer. The application of the contact surfaces causes geometrical nonlinearity and extends the time of calculations but it also has two important advantages. First, it provides theoretically infinite mutual displacements of interacting bodies without causing large distortions of finite elements at the contact. Second, the solution enables one independent FE meshing of both the bodies which is convenient in the case of bodies with various geometry and finite element sizes.

An original semi-micro-modelling of masonry is applied to the arch barrel. The masonry arch is divided into even segments which represent pieces of masonry consisting of several bricks or stones. The segments are separated by individual mortar joints of weaker material comprising predefined planes of weakness. An analogical approach was used earlier in 2D models of masonry arch bridges (Ford et al. 2003, Bień and Kamiński 2006). The assumed thickness of all

mortar joints is 3 cm. The number and configuration of the segments in both directions of the arch plane is analysed below. Quite a simple problem is the division in the longitudinal direction which corresponds to the division in the already mentioned 2D models. In this case the transverse joints in FE model exactly coincide with selected bed joints of real single-ring masonry arches. A more complicated situation arises in the transverse direction where, due to the presence of a masonry bond, head joints do not lay in common planes. The shape of a potential path of cracking is dependent on the applied masonry bond. A few masonry bond styles are shown in Fig. 2 with potential cracking paths indicated with grey bold lines. Regarding the bending moment as a dominant force causing cracking of the masonry arch bond, it is proposed that the substitution of bigger segments (black dashed lines) for the original masonry should take into account unit bending strength of the arch in the considered direction. For simplification the arch is treated as a plane wall for which, neglecting the tensile strength of mortar joints, bending strength in the direction parallel to the bed joints is determined only by the torsion strength of the bed joints. The axis of mutual rotation of both separated parts lays on the surface of the masonry as shown in Fig 2.

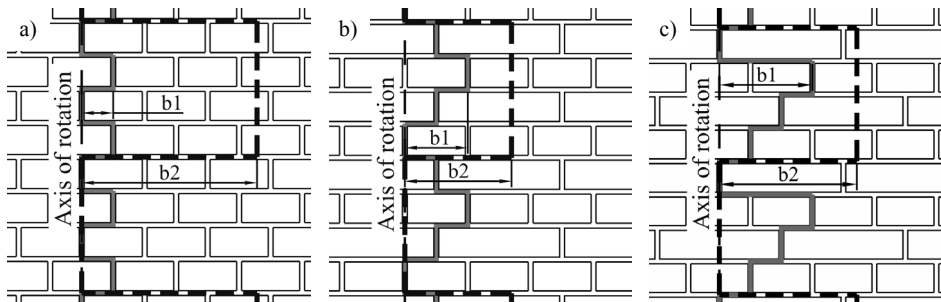


Figure 2 : The original masonry bonds with potential cracking paths (grey lines) and new bond patterns (black dashed lines) for various bond styles: Header (a), English (b) and Dutch (c).

According to the assumption presented above, the new bond of masonry segments should provide the same torsion strength of the bed joints. It can be done by the adjustment of the segment width (in the transverse direction) to give the bed joints proper value of the torsion strength. The torsion strength T of a cross-section is equal:

$$T = t\mu N \quad (1)$$

where t = coefficient of torsion strength, μ = coefficient of friction and N = axial force.

Assuming the same coefficient of friction and a normal force acting in the cross-section, the calculation can be limited to a comparison of the coefficients of torsion strength: t_1 for the original bed joints included on the length of the new masonry segment and t_2 for a single bed joint of the new segment. The coefficient of torsion strength t for a rectangular cross-section taken about one of its vertices can be calculated with the formula proposed by Orduna and Lourenco (2005):

$$t = \frac{1}{3} \left[c + \frac{a^2}{2b} \cdot \ln\left(\frac{b+c}{a}\right) + \frac{b^2}{2a} \cdot \ln\left(\frac{a+c}{b}\right) \right] \quad (2)$$

where: a , b = sides of the rectangle and c = diagonal of the rectangle ($c = \sqrt{a^2 + b^2}$).

Replacing b in Eq. (2) with b_1 for the original bond and with b_2 for the new bond (according to Fig. 2) and taking a equal to the arch thickness d , the corresponding t_1 and t_2 values can be received. The unknown b_2 value can be found from the equality of the torsion strengths:

$$nt_1 = t_2 \quad (3)$$

where n = assumed number of bed joints of width b_1 of the original masonry within the range of a single segment of the new masonry bond.

For the assumed divisions in the longitudinal direction presented in Fig. 2 (giving four times longer segments than the original brick height) the corresponding values of n are 4 for the Header bond and 2 for both English and Dutch styles. Interestingly enough, the highest torsion strength calculated in the proposed way for the assumed cracking paths is for the Header bond style being about twice as big for the English one. For the presented model the division into 20 segments in the longitudinal and 8 in the transverse direction was assumed.

The spandrel walls and the backfill are created by means of the macro-modelling technique as continuous areas of a homogenous material with no special features.

The live load is applied to a rigid plate with dimensions 50x100 cm acting on the top surface of the soil by means of a contact surface. Such a solution enables one to apply conveniently the load in any position without limiting the transverse displacements of the soil under the loading plate. In the presented analyses the load is located at the quarter of the span and at 3/8 of the structure width. The boundary conditions imposed on the rigid body constrain its horizontal translations and the rotation about the vertical axis.

2.3 FE mesh

The applied FE mesh topology requires a special description. The presented strategy assumes a minimum number of elements providing a good representation of potential global failures of the structure. Meshing of the arch barrel was analysed with two patterns presented in Fig. 3a,b. Finally, the pattern in variant 2 (Fig. 3b) was selected as the one with less distorted joint elements. The number of elements along the arch thickness is reduced to 3 to obtain an acceptable size of the numerical problem. However, it is probably slightly too small a value to provide a very precise distribution of stresses along the arch thickness. In the whole arch barrel 8-node linear hexagonal elements were applied. Due to the connection of the arch barrel with the spandrel walls, the edges of head joints are situated on the internal surfaces of the spandrel walls to obtain a decent mesh in both elements. Therefore, also the number of elements along the spandrel wall thickness is equal to the number of elements in the edge masonry segment of the arch. A detail of this connection is presented in Fig. 3c. Meshing of the soil is independent of the mesh of other structural parts, however, it is thickened at the boundary with the arch to make the interaction between the components more precise. In both the spandrel wall and the soil the FE mesh density decreases with the increasing distance from the arch due to lower importance to the solution of the more distant elements. In both the spandrel wall and the soil hex-dominated meshing is applied using 6-node linear triangle prisms or 8-node linear hexagons. The total number of nodes is over 30 thousand, which gives about 90 thousand variables.

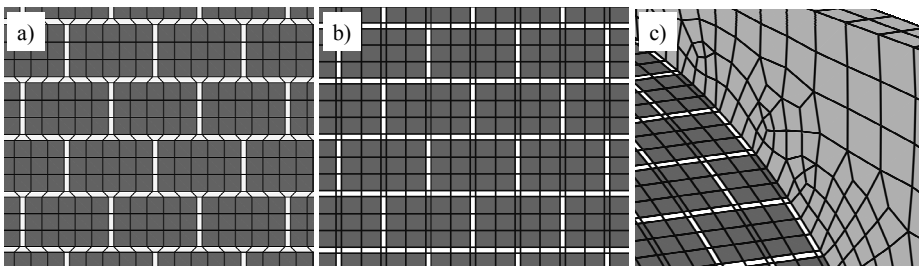


Figure 3 : Details of FE mesh pattern of the arch barrel in variant 1 (a), variant 2 (b) and connection of the arch with the spandrel wall (c).

2.4 Model of material

The applied constitutive models of the materials take into account the behaviour of the structure before and after reaching the limit state. As already mentioned, the model of the arch barrel is composed of two types of material: masonry blocks and mortar joints. The first one is defined as a linear elastic isotropic material with modulus of elasticity equal to $E_b = 10$ GPa representing average characteristics of the masonry segment components. The mortar joints are modelled as a concrete-like material (according to ABAQUS Documentation – Hibbit et al. 2005) which

considers plasticity with strain softening in both compression and tension. Modulus of elasticity of the mortar is $E_m = 1$ GPa. Initial yield stresses in uniaxial tension and in uniaxial compression are equal 0.1 MPa and 6 MPa respectively. The model assumes nonassociated plastic flow with the dilation angle equal 33° . Unit weight of both masonry materials is 20 kN/m^3 . All material characteristics of the spandrel walls are assumed the same as for the mortar joints, i.e. are corresponding to the properties of concrete. The backfill material represents granular soil with the modulus of elasticity $E_s = 200$ MPa, angle of internal friction $\phi = 45^\circ$ and cohesion $c = 30$ kPa. Yield surface for the soil is defined by linear Drucker-Prager model; plastic flow is nonassociated with the dilation angle equal to 20° . Unit weight of soil is equal to 18 kN/m^3 .

3 NUMERICAL ANALYSES

3.1 Analysis procedure

The applied approach to the solution of the FEM problem is the implicit method. Naturally, due to geometry and material definitions presented in the previous chapter, the analysis is strongly nonlinear, based on the large displacement theory and uses unsymmetrical stiffness matrix. The solution runs incrementally in two consecutive steps: in the first one self weight of all structural components is applied, in the second one the live load acting through the rigid plate is added. The incremental application of the live load is controlled by means of the vertical displacement of the rigid plate. Such a solution gives a better control over the development of the global failure of the structure and enables one to reach and exceed the ultimate limit state which comprises the goal of the analysis. The ultimate load is defined by the highest value of the load taken from the relationship between the vertical displacement u and force P acting on the rigid body. In the analysed cases a sufficient displacement of the plate to reach the limit state is ca. 30 cm. The number of increments is about 20 for the first step and at least 300 for the second step. The real time of the solution is about 40 hours. The calculations were carried out by means of a single computer with Itanium2 1.4 GHz processor and 2 GB RAM memory.

3.2 Results for full 3D model

In this chapter results for a full 3D model of the masonry bridge described in Section 2 are presented in the form of the ultimate load value and the mode of failure. The ultimate load defined by the highest point on the P - u diagram shown in Fig. 4 is equal to $P_{ult}^f = 591.9$ kN. The peak value is reached at relatively large displacement of the loading plate equal to $u = 34$ cm. It is visible from Fig. 4 that at the beginning of the loading process the slope of the P - u curve is quite steep (area A). Then after reaching the soil yielding and after exceeding the limit friction at the contact between the arch barrel and soil the curve is more gradual (area B). It becomes steeper again when a bigger area of the soil is mobilised to restrain the increasing

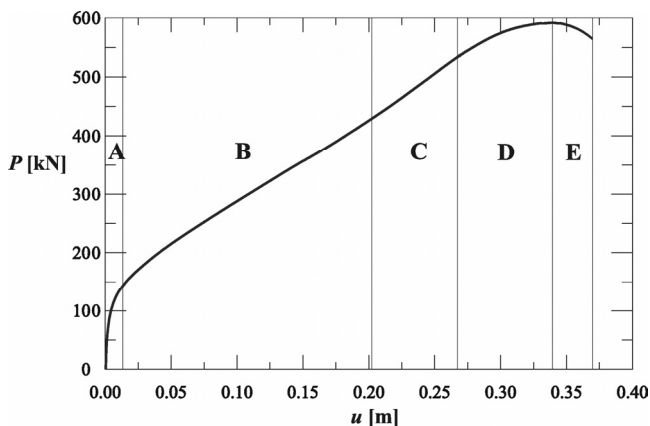


Figure 4 : The P - u relationship for the loading plate with the areas of changing behaviour.

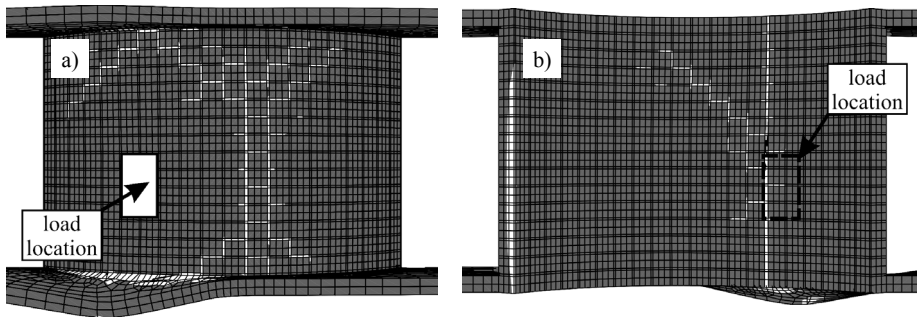


Figure 5 : The global mode of failure with maps of plastic strains presented for the bare arch of the full 3D model with the load location indicated: top view (a) and bottom view (b).

deformation (area C). Finally, the following drop of the structural stiffness (area D) is already related to the cracking of the arch barrel and formation of the mechanism what defines the limit state of the whole system. The last descending part of the curve (area E) represents a post-failure behaviour corresponding to the collapse of the structure. The foregoing description is only a simplified interpretation of P - u relationship because there are neither clear nor common instants of the yield beginning for every structural component, and the effect is fuzzy over time and the structure space. However, it shows general dominant tendencies of the structural material during the loading process.

Important and interesting information is also the global mode of failure of the structure presented in Fig. 5. It is significantly different from and more complex than those possible to obtain by means of 2D models. The general tendency to form a four-hinge mechanism is visible but the failure mode shows also diagonal cracking of the arch barrel. This effect is caused by the stabilising influence of the spandrel walls restraining creation of cracks in the extrados of the arch at its edges. A significant advantage of the model is that the proposed division of the masonry into segments provides analysis of diagonal cracks probable to appear in real structure.

3.3 Three-dimensional models for symmetrical problems.

In the case of both structure geometry and loading scheme symmetrical about the longitudinal axis a reduced half-model can be applied. It is composed of half of the structure, thus the number of finite elements is decreased twice which significantly reduces computational effort. The only difference in discretization of the structure with respect to the full model appears in the area of the plane of symmetry. Due to the division of the structure, one row of the mortar head joints lays exactly in the plane of symmetry. Therefore, it should be divided in the middle as shown in Fig 6a (variant A). However, it creates very narrow elements with improper side ratio which undergo a large distortion during loading. Alternative solutions, presented in Fig. 6b,c eliminate the problem of weak mortar elements in the plane of symmetry. In the analysis presented here the second discretization approach (variant B - Fig. 6b) was assumed. The boundary conditions in the longitudinal plane of symmetry constrain translation normal to the plane and both out-of-plane rotations. The exemplary deformed configuration of the arch and spandrel walls with the maps of plastic strains is shown in Fig. 7.

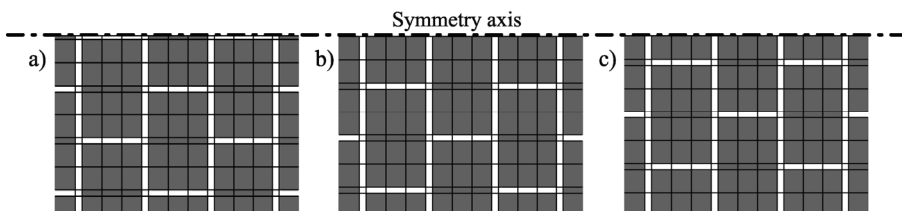


Figure 6 : The details of FE mesh pattern at the plane of symmetry in variants: A (a), B (b) and C (c).

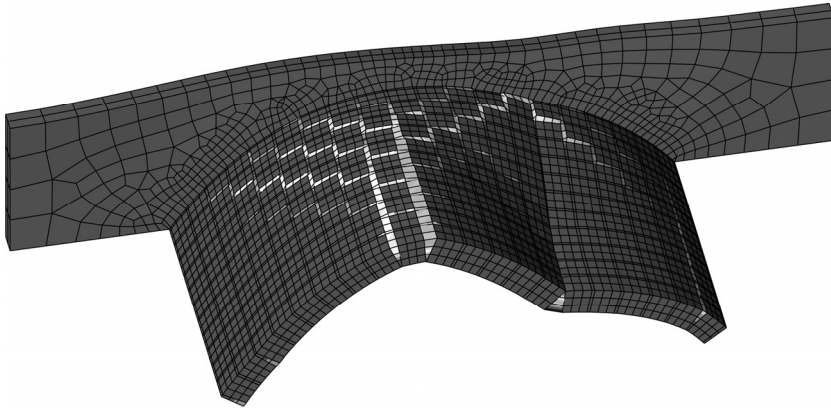


Figure 7 : The global mode of failure with maps of plastic strains for the half-model.

3.4 Three-dimensional models neglecting spandrel walls

A further simplification for 3D modelling of masonry bridges assumes elimination of the spandrel walls. It is a safe assumption which can be realistic for wide structures loaded centrally on a narrow path where punching through the arch barrel can be a dominating failure mode or when the spandrel walls do not cooperate with the arch properly. The latter case takes place, e.g. when there is a fracture between the spandrel wall and the arch barrel. Both lateral surfaces of the model have imposed constraints on the normal to the plane translation and both out-of-plane rotations. An example of such a model with mesh variant I (Fig. 3a) is shown in Fig. 8.

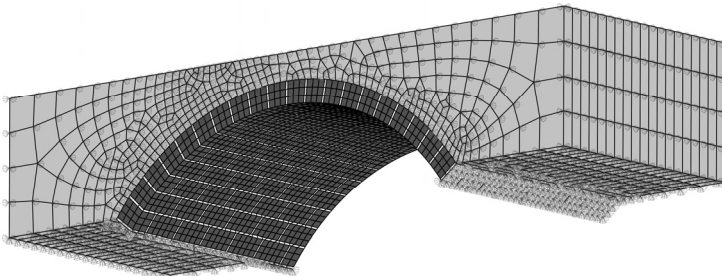


Figure 8 : A simplified 3D model without spandrel walls.

3.5 Comparison with 2D analyses

Useful information can be received from the comparison of the presented 3D model with 2D model created on the basis of analogical assumption – with the application of predetermined planes of weakness (Bień and Kamiński 2006). Of course, planes of weakness considered in 2D model comprise only the bed joints of the arch; any transverse effects or the influence of spandrel walls cannot be analysed in models of this type. The model analysed here has geometrical parameters corresponding to those given in Section 2. In the transverse direction the elements have a unit width and work in a condition of plane strains. The results of the analysis carried out by means of 2D and 3D models are compared in Fig. 9 by deformed configurations of the structures with maps of plastic strains at the limit state. It can be noticed that 2D model, though it does not provide the information on the transverse behaviour, quite well locates four plastic hinges appearing in the plane of symmetry in 3D model.

The results of the analyses carried out by means of 2D and 3D models for various structure geometries are presented in Table 1 in the form of the ultimate loads: the total values P_{ult} and the values per 1 m width of structure P_{ult}^l . The results indicate that in the assumed loading scheme the ultimate load obtained from 2D model is slightly higher than the unit value P_{ult}^l for 3D models and is closer to the values for narrower structures.

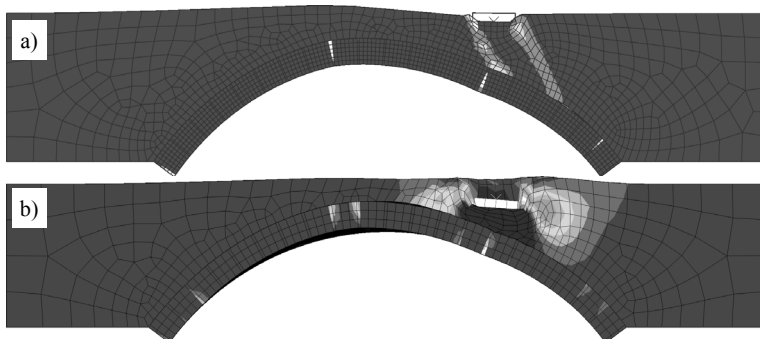


Figure 9 : The comparison of the deformed configurations of 2D (a) and 3D (b) models with maps of plastic strains.

Table 1 : Ultimate loads for the analysed models.

Model dimension	3D	3D	3D	2D
B [m]	4.0	6.0	8.0	1.0
P_{ult} [kN]	734.6	976.6	1055.0	191.5
P_{ult} [kN/m]	183.7	162.8	131.9	191.5

4 CONCLUSIONS

The proposed 3D model, unlike any 2D models, enables one an advanced analysis of masonry arch bridges taking into account transverse effects. The simplified discretization of the arch barrel based on a careful FE modelling can imitate behaviour of various masonry types at the limit state. The analyses using the proposed models are time consuming but possible to carry out with an acceptable effort. The problems can be also easily reduced making use of the structure symmetry. The proposed models deliver important data on the failure modes, significantly different from those given by 2D models. According to the results, the ultimate load increases with the bridge width but the relationship is not proportional. The presented 3D model can be useful for calibration of the results received by means of simpler 2D models.

ACKNOWLEDGEMENTS

The present study is partly supported by *Sustainable Bridges* project within the 6th Framework Programme of the European Union. All calculation were carried out by means of ABAQUS 6.5 at WCSS of Wroclaw University of Technology. These supports are gratefully acknowledged.

REFERENCES

- Bień, J. and Kamiński T. 2006. Numerical modelling of damaged masonry arch bridges. In P.J.S. Cruz, D.M. Frangopol and L.C. Neves (eds), *Bridge Maintenance, Safety, Management, Life-Cycle Performance and Cost; Proc. of the 3rd intern. conf., 16-19 July 2006*, p. 227-228.
- Fanning, P.J. and Boothby, T.E. 2001. Three-dimensional modelling and full-scale testing of stone arch bridges, *Computers & Structures* 79, p. 2645-2662.
- Ford, T.E., Augarde, C.E. and Tuxford, S.S. 2003. Modelling masonry arch bridges using commercial finite element software, *9th International Conference on Civil and Structural Engineering Computing, 2-4 September 2003*. Egmond aan Zee.
- Hibbit, Karlsson and Sorensen Inc. 2005. *ABAQUS 6.5 Documentation*.
- Lourenco P.B., Rots J.G. and Blaauwendraad J. 1995. Two approaches for the analysis of masonry structures: Micro and macro-modelling. *HERON* 40(4), p. 313-340.
- Orduna, A. and Lourenco, P. B. 2005. Three-dimensional limit analysis of rigid blocks assemblages. Part I: Torsion failure on frictional interfaces and limit analysis formulation. *International Journal of Solids and Structures* 42, p. 5140-5160.